Water Science & Technology

Water Science & Technology Vol 00 No 0, 1 doi: 10.2166/wst.2024.199

Effect of biochar addition on the anaerobic digestion of food waste: microbial community structure and methanogenic pathways

Siyao Pei[a], Xiaodan Fan[a,b], Chunsheng Qiu[a,b], Nannan Liu[a,b,*], Fei Li[a], Jiakang Li[a], Li Qi[a,b] and Shaopo Wang[a,b]

[a] School of Environmental and Municipal Engineering, Tianjin Chengjian University, Tianjin 300384, China
[b] Tianjin Key Laboratory of Aqueous Science and Technology, Tianjin 300384, China
*Corresponding author. E-mail: lnn979@126.com

ABSTRACT

This study assessed the effects of the addition of biochar prepared at 700 °C with different dosages on the anaerobic digestion of food waste. The biochar addition at a concentration of 10.0 g/L increased the cumulative methane yield by 128%, and daily methane production was also significantly promoted. The addition of biochar derived from poplar sawdust significantly increased the relative abundance of dominant bacteria for anaerobic digestion by 85.54–2530% and promoted the degradation of refractory organic matter and the transfer of materials between the hydrolysis and acid production stages. Further analysis has demonstrated that *Bathyarchaeia* and hydrogenotrophic methanogens were enriched by the biochar addition. Meanwhile, the relative abundances of functional genes, including C5-branched dibasic acid metabolism, and pyruvate metabolism, were increased by 11.38–26.27%. The relative abundances of genes related to major amino acid metabolism, including histidine metabolism, lysine biosynthesis, and phenylalanine, tyrosine, and tryptophan biosynthesis, were increased by 11.96–15.71%. Furthermore, the relative abundances of genes involved in major replication and repair were increased by 14.76–22.76%, and the major folding, sorting, degradation, and translation were increased by 14.47–19.95%, respectively. The relative abundances of genes related to major membrane transport and cell motility were increased by 10.02 and 83.09%, respectively.

Key words: anaerobic digestion, carbohydrate and amino acid metabolism, hydrogenotrophic methanogens, poplar sawdust

HIGHLIGHTS

- Different dosages of biochar in the anaerobic digestion process of food waste were studied.
- 16S rRNA gene sequencing and PCR were used to analyze bacterial and archaeal domains.
- The addition of biochar has promoted the improvement of anaerobic digestion performance, e.g. the improvement of methane production capacity, the increase of anaerobic digestion-dominant bacterial communities, and the abundance of functional genes.

GRAPHICAL ABSTRACT

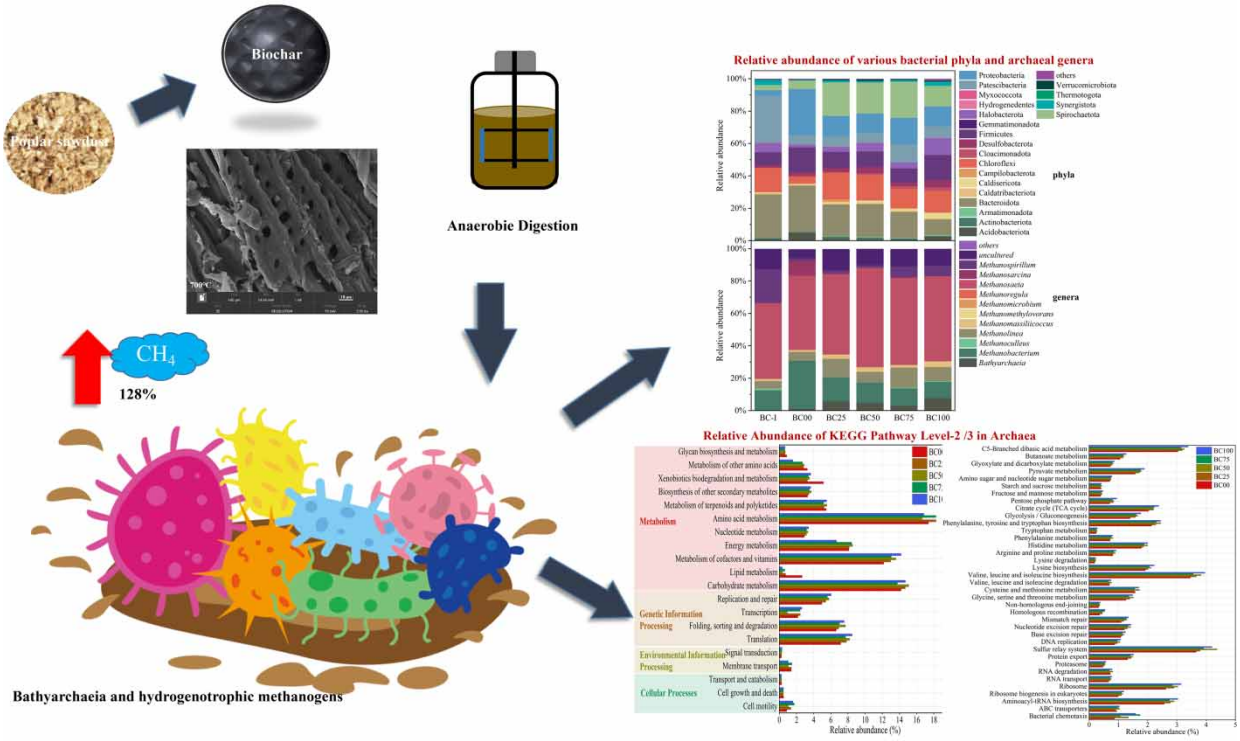

1. INTRODUCTION

The growing production of food waste, containing food residues, grains, and vegetables, has become a major challenge for municipal solid waste treatment and disposal (Devi *et al.* 2023; Liu *et al.* 2023). Improper treatment and disposal of food waste may cause serious environmental burdens, such as land use, greenhouse gas emissions, and groundwater pollution risk (Gu *et al.* 2022; Liu *et al.* 2023). As a waste-to-energy technology, the anaerobic digestion of organic wastes has attracted widespread attention (Devi *et al.* 2023). However, as anaerobic digestion is a complex biological process, the high organic content of food waste could cause acidification, ammonia nitrogen inhibition, and consequently low process efficiency (Li *et al.* 2018a; Rasapoor *et al.* 2020).

Biochar is a highly aromatic carbon-rich product with a well-developed pore structure, a high specific surface area, and abundant oxygen-containing functional groups and can be prepared by the thermal conversion of biomass under oxygen-depleted conditions (Visiy *et al.* 2022; Valenzuela-Cantú *et al.* 2024). As an additive material, biochar has been widely used to improve anaerobic digestion performance, such as increasing methane yield, improving system stability, shortening hysteresis, and improving biogas quality through buffering effect, direct interspecific electron transfer, microbial immobilization, and disinhibition (Wang *et al.* 2021a; Chen *et al.* 2023; Valenzuela-Cantú *et al.* 2024). Wang *et al.* (2021a) revealed that the biochar addition in the process of anaerobic co-digestion of food waste and dewatered activated sludge could enrich the electroactive *Syntrophomonas* and *Methanosarcina*. As a potential redox-active medium, biochar can stimulate the potential direct electron transfer between species and inhibit the hydrogen synthase pathway (Wang *et al.* 2021a). Cui *et al.* (2021) found that biochar addition could increase the relative abundance of bacteria involved in syntrophic interactions, such as *Syntrophomonas* and *Syntrophobacter*, under high ammonia stress. Wang *et al.* (2021c) confirmed that methane production increased by 35–37% when the dosage of biochar increased from 0.6 to 1.2 g/g-TS in the algae anaerobic digestion process. However, the excess biochar may inhibit the growth of methanogens due to the alkali metals and functional groups on the surface (Shen *et al.* 2016). Shen *et al.* (2016) found that the cumulative methane production with the biochar addition of 12 g/L was 18.25% higher than that with a biochar dosage of 50 g/L. Luo *et al.* (2022) also demonstrated that the highest specific methane production of 553.0 mL/g-VS had been gained with a biochar dosage of 10 g/L rather than a higher dosage. However, Altamirano-Corona *et al.* (2021) found that the methane yield with a biochar dosage of 10 g/L had decreased by 10.7% with the control group.

Therefore, this study aimed to investigate the effects of biochar addition with different dosages on the anaerobic digestion process of food waste. The effect of biochar addition on methane yield was evaluated, and the changes in microbial community structure and methanogenic pathways were also explored.

2. MATERIALS AND METHODS

2.1. Preparation and characteristics of biochar

Poplar sawdust, purchased from Lianyungang City (China), was selected as the feedstock for biochar preparation. Biochar was prepared through the pyrolysis of poplar sawdust in a muffle furnace at 700 °C for 2 h under oxygen-limited conditions (Shanmugam *et al.* 2018). The yield of biochar is the mass ratio of biochar to initial dry biomass (Yang *et al.* 2020a, 2020b). The pH value of biochar was measured in a 10% (W/V, weight/volume) suspension in ultrapure water prepared by shaking at 150 rpm under ambient temperature for 24 h using a pH meter (PHB-4, LEICI, China, Xu *et al.* 2020). Ash contents were determined using the ASTM method (D-1762-84, Bagul *et al.* 2017). A scanning electron microscope (SEM, MIRA LMS, TESCAN, The Czech Republic) was used to observe the surface morphology of biochar. Energy-dispersive spectroscopy (Xplore 30, Oxford, UK) was used to examine the elemental composition of biochars. An automated surface area and Porosity Analyzer (TriStar II 3020, Quantachrome, USA) were used to determine the Brunauer–Emmett–Teller (BET) surface area and the pore structure of biochars. Fourier transform infrared (FTIR) (TENSOR-27, Bruker, Germany) was used to analyze the functional groups of biochars.

2.2. Substrate and inoculum

The food waste used in this study was composed of rice (20%), meat (20%), vegetables (30%), legumes (15%), and fats (15%) (Fisgativa *et al.* 2016). An anaerobic digestion inoculum (total solids (TS) of 10.98 $\pm$ 0.25 g/L, volatile solids (VS) of 6.65 $\pm$ 0.15 g/L) was collected from a laboratory-scale continuous stirred tank reactor that operates stably at 35 $\pm$ 1 °C for the anaerobic digestion of sewage sludge.

2.3. Batch food waste anaerobic digestion experiments

An automatic biomethane potential testing system (AMTPS-II, Bioprocess Control Company, Sweden) was used to perform anaerobic digestion batch experiments. A total of 400 mL digesters are filled with 300 mL of inoculum sludge and 10.71 g of food waste, and then biochar with the dosages of 0 g/L (BC00), 2.5 g/L (BC25), 5.0 g/L (BC50), 7.5 g/L (BC75), and 10.0 g/L (BC100) was added, respectively. Each test was made in triplicate; all bottles were added with distilled water to a constant volume of 400 mL and sealed. Subsequently, nitrogen was introduced into all batch digesters to keep an anaerobic state. Then, all digesters were cultured under 35 $\pm$ 1 °C until no biogas was produced. The specific meanings of some of the abbreviations used in this paper are given in Table S1 of the Supplementary Material.

2.4. Analytical methods

pH, TS, VS, and ammonia nitrogen of the mixed culture were measured according to standard methods (Yirong *et al.* 2017). 16S rRNA gene sequencing and polymerase chain reaction (PCR) amplification were used to analyze bacterial and archaeal domains. The mixed culture samples of BC00, BC25, BC50, BC75, and BC100 were collected from the digesters at the end of the anaerobic digestion process. Then, samples were stored at −20 °C before being delivered to Allwegene Co., Ltd (Allwegene, Beijing, China) for high-throughput sequencing. PCR extraction of these samples was performed using the Agencourt AMPure XP as per the manufacturer's instructions. The V3–V4 hypervariable regions of 16S rRNA from bacteria and archaea were amplified using universal primer sets of 338–806 (ACTCCTACGGGAGGCAGCAG, GGACTACHVGGGTWTCTAAT) and 344–806 (ACGGGGYGCAGCAGGCGCGA, GGACTACVSGGGTATCTAAT), respectively. Subsequently, the Illumina MiSeq was used to sequence PCR products. The Kyoto Encyclopedia of Genes and Genomes (KEGG) database was used to analyze the functional gene prediction pathways.

3. RESULTS AND DISCUSSION

3.1. Physicochemical properties of biochars

SEM images (Figure 1) showed that biochar was composed of irregularly shaped particles with highly porous structures and rough surfaces due to the escape of volatile gases during carbonization (Das *et al.* 2021). Biochar had a micro-pore volume of 0.01 cm^3/g, a total pore volume of 0.08 cm^3/g, and a BET surface area of 297.68 m^2/g (Table 1). The large surface area and

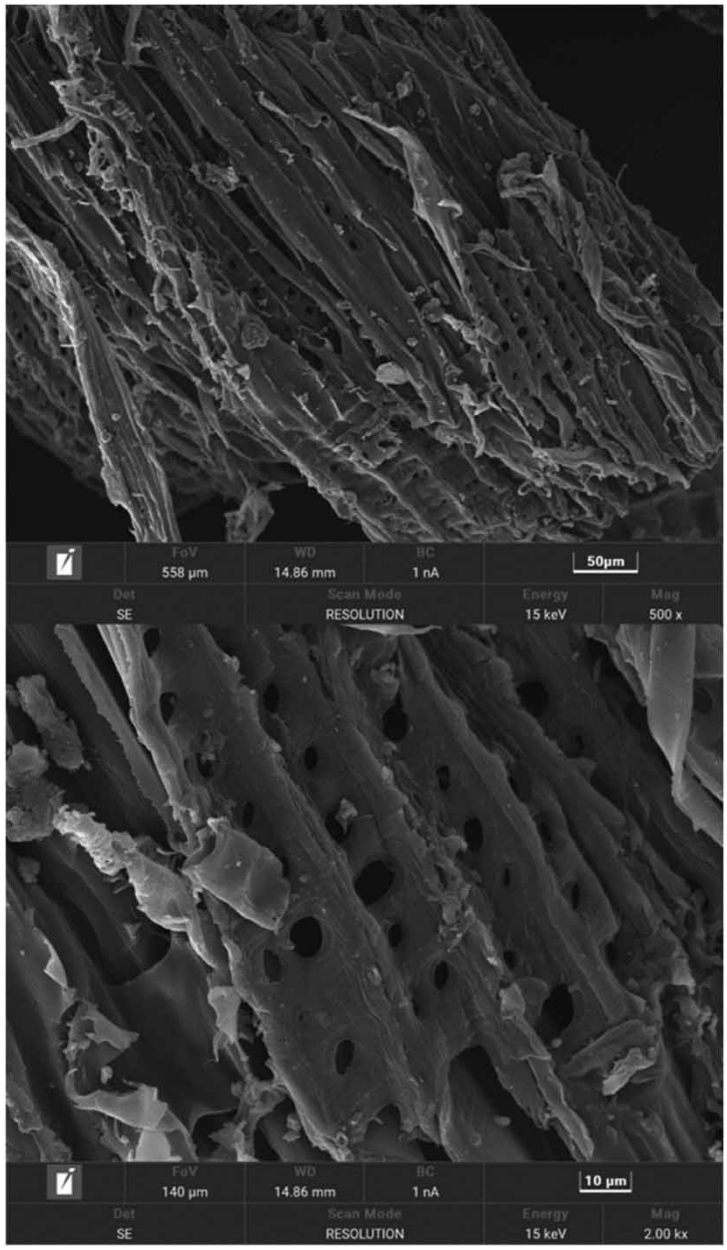

Figure 1 | SEM of biochar (500 and 2,000 times).

the excellent porous structure of biochar could create favorable conditions for the formation of microbial biofilms and provide a suitable surface for acid adsorption (Pan *et al.* 2019). The carbon content of biochar was 85.21%, and a high carbonization degree usually results in relatively high conductivity (Sun *et al.* 2017; Lam *et al.* 2018).

The FTIR spectra of biochar is presented in Figure 2. The absorbance peaks at wavenumbers of 3,416–3,405, 3,000–2,800, and 2,300–1,900 cm^{-1} were due to the stretching vibration of hydroxyl groups O–H (Xin *et al.* 2017), C–H of aliphatic compounds (Hu *et al.* 2021), hydroxyl and carbonyl functional groups, respectively. Wang *et al.* (2021b) found that biochars with high absorption peaks of redox-active organic functional groups (such as O–H, C = O, and C–H) usually showed good ability to act as a shuttle or electron mediator. The absorbance peaks at wavelength of 1,400–1,240 cm^{-1} were due to the presence of the ether group (C–O–C) in cellulose (Das *et al.* 2009). The absorbance peaks at wavenumbers of 1,612 and 1,260–1,100 cm^{-1}were the characteristic peaks of quinone C = C or C = O (Zhang *et al.* 2019) and associated with the presence of phenazine (Shanmugam *et al.* 2018). The reversible electron transfer capacity of electroactive oxygen functional groups (quinone

Table 1 | Physio-chemical characteristics of biochar

Analysis	Parameter	Biochar
Proximate analysis	Biochar yield (wt. %)	26.88 ± 0.10
	Ash content (wt. %)	21.64 ± 0.56
Physio-chemical	pH	9.72 ± 0.01
Property	BET surface area (m^2/g)	297.68
	Micro-pore volume (cm^3/g)	0.01
	Total pore volume (cm^3/g)	0.08
Ultimate analysis	C (wt.%)	85.21
	O (wt.%)	12.18
	Na (wt.%)	0.08
	Mg (wt.%)	0.19
	K (wt.%)	0.81
	Ca (wt.%)	1.26
	Mn (wt.%)	0.07
	Fe (wt.%)	0.2

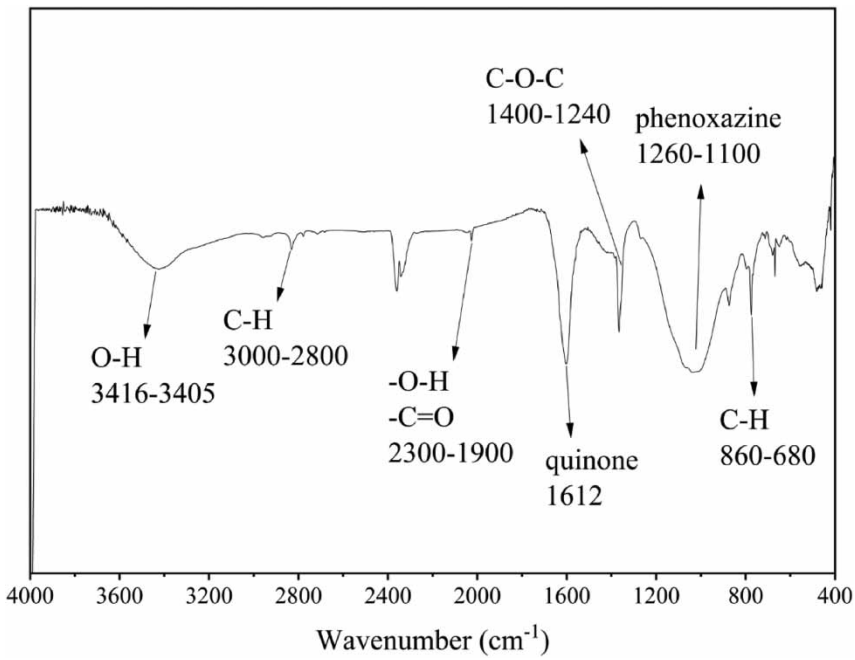

Figure 2 | FTIR spectra of biochar.

and phenazine) on biochar surfaces could promote potential direct interspecies electron transfer (DIET) for the degradation of volatile fatty acids (Binh & Kajitvichyanukul 2019; Wang *et al.* 2020a). The absorbance peaks at wavelength of 860–680 cm^{-1} were due to the stretching vibration of the aromatic C–H bond (Wang *et al.* 2020b).

3.2. Effect of biochar addition on anaerobic digestion

3.2.1. Variation of pH and NH_3-N concentration in the anaerobic digestion system

The pH values and NH_3-N concentrations during the anaerobic digestion process are shown in Figure 3. The pH of all groups reached its lowest values on the third day and then gradually increased until the end of the test. The pH values of the test groups were higher than those of the control group, probably because the addition of biochar could provide carriers for

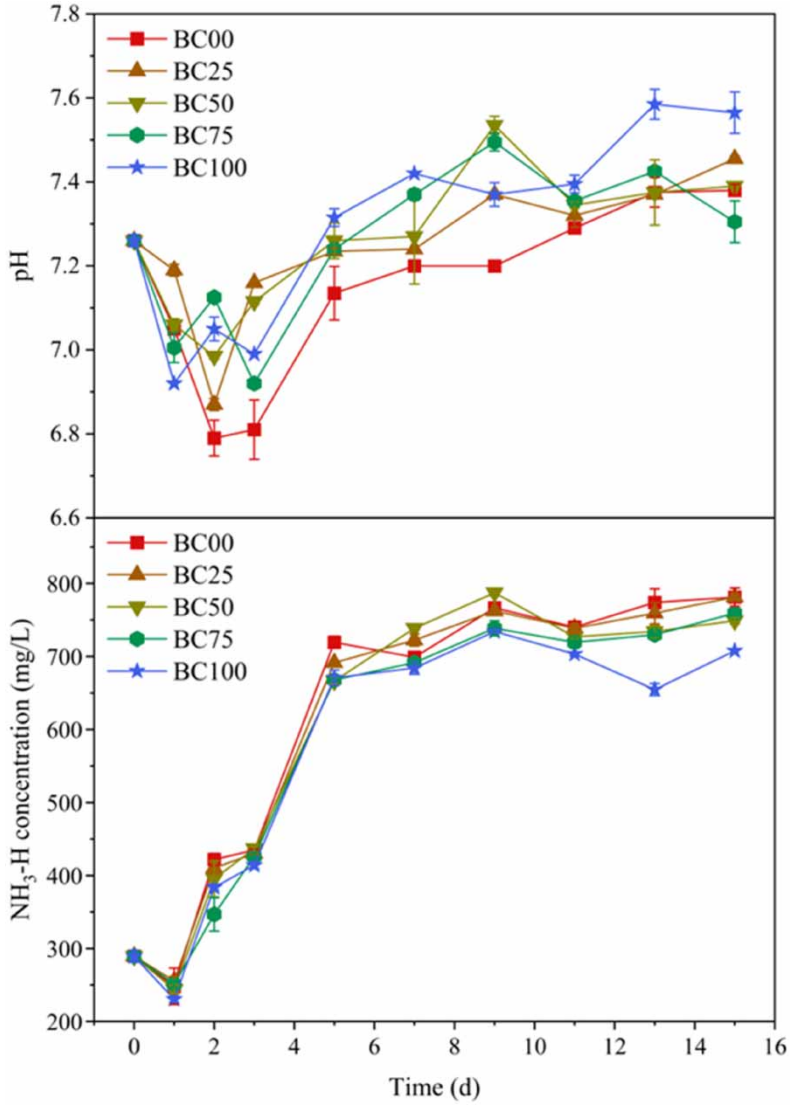

Figure 3 | pH value and NH_3-N concentrations vary with time.

microorganisms and promote the growth of methanogens, thereby accelerating the consumption of organic acids. In addition, the presence of a large number of alkaline groups (Figure 2) and alkali or alkaline earth metals (Table 1) could also play a buffering role (Luo *et al.* 2015). The pH value of the BC100 group was relatively higher than the other groups, which could mitigate the effect of volatile fatty acid accumulation on methanogenic microbes. The NH_3-N concentration was between 230.57 and 781.34 mg/L. The NH_3-N concentration in BC100 was lower than in the other groups, which could be attributed to the fact that biochar addition could promote the growth and reproduction of the microbes that consume NH_3-N (Luo *et al.* 2015).

3.2.2. Profiles of methane production

Figure 4 shows the effect of biochar addition on methane production. The highest cumulative methane volume was 759.35 ± 13.15 mL for BC100, followed by BC50 (397.50 ± 28.80 mL), BC25 (393.03 ± 1.79 mL), BC75 (384.7 ± 0.30 mL), and BC00 (332.5 ± 0.50). The cumulative methane production of each experimental group showed the same trend in the first 5 days, and methane was produced mainly from small molecular and easily degradable organic matter. BC00, BC25, BC50, and BC75 showed significant biogas production peaks on the second day, which were 218.00, 243.60, 247.20, and 197.00 mL/d, respectively. BC100 had two significant biogas production peaks, 218.00 (day 2) and 89.60 mL/d (day 10). The first peak of

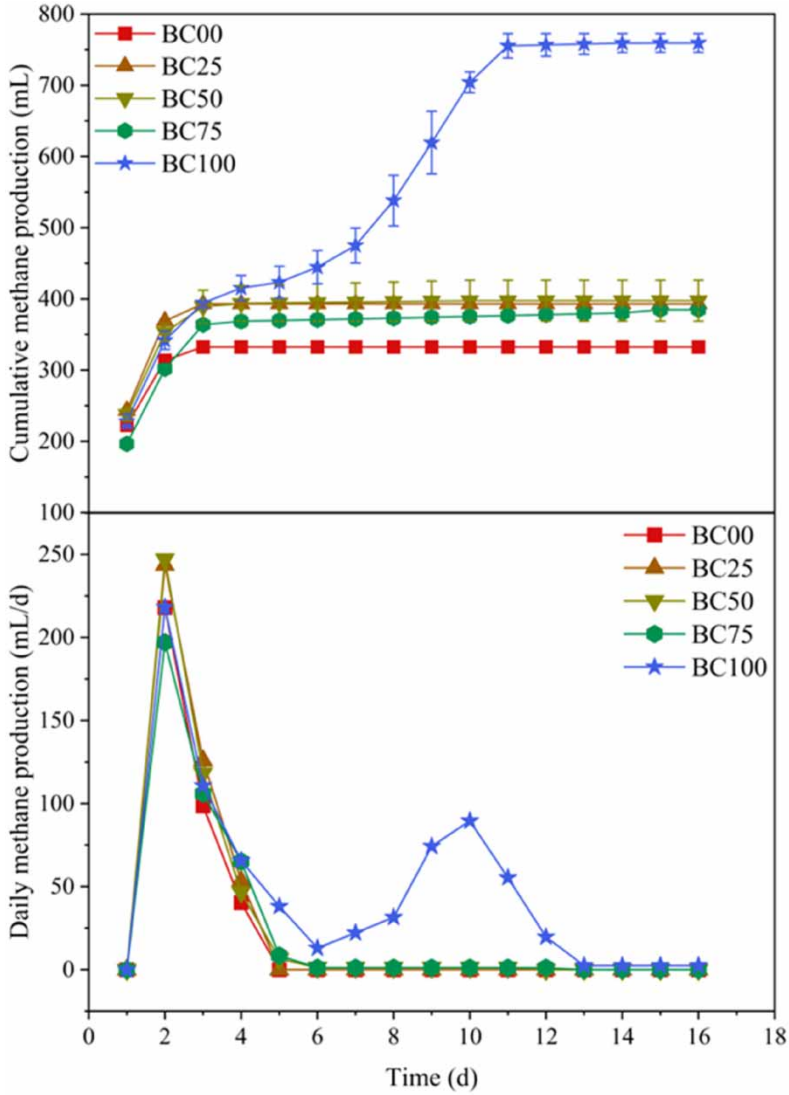

Figure 4 | Cumulative and daily methane production varies with time.

biogas production was mainly due to the digestion of degradable substances by methanogenic bacteria (Kaur *et al.* 2020). At the same time, macromolecular organic matter was decomposed into organic acids through hydrolysis and acidification, which led to a decrease in pH value (Figure 3), and the daily methane production dropped sharply in the following days. The daily methane production of BC100 was significantly higher than that of other groups in the late stage of the anaerobic digestion process, mainly due to the digestion of refractory macromolecular organic matter.

3.2.3. Microbial community structure

The microbial community structures of different experimental groups are shown in Figure 5. Bacteroidetes are often associated with the decomposition and fermentation of polysaccharides (Rivière *et al.* 2009; Lim *et al.* 2020). The relative abundances of Bacteroidetes decreased by 31.10% (BC25), 28.40% (BC50), 43.50% (BC75), and 65.93% (BC100), respectively, compared with that in BC00, mainly due to the components of the substrate having a relatively low content of polysaccharide. Meanwhile, the addition of biochar increased the relative abundance of Chloroflexi. Chloroflexi could degrade monosaccharides and polysaccharides with the production of acetic acid (Rivière *et al.* 2009). The relative abundances of Chloroflexi in BC25, BC50, BC75, and BC100 increased by 271.61, 252.72, 169.54, and 197.63%, respectively, compared with that in BC00.

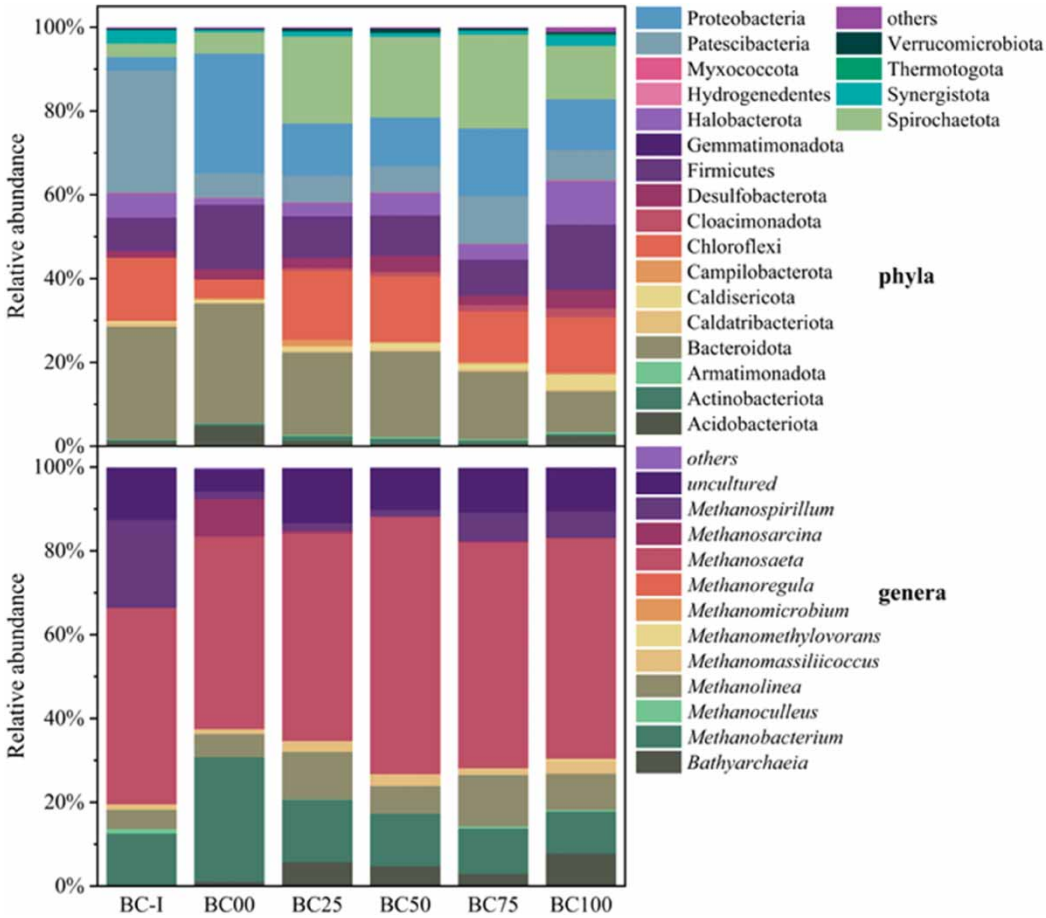

Figure 5 | Relative abundance of various bacterial phyla and archaeal genera.

Firmicutes can produce extracellular enzymes (such as cellulase, lipase, and protease) and play an important role in the catabolic metabolism of cellulose, lipids, proteins, sugars, and amino acids (Zhao *et al.* 2017). The relative abundances of Firmicutes in BC25, BC50, and BC75 decreased by 36.58, 37.62, and 44.21%, respectively, compared with that in BC00, while that in BC100 increased by 1.76%. Biochar addition increased the relative abundance of Halobacterota, Hydrogenedentes, Patescibacteria, Spirochaetota, and Synergistota. Halobacterota includes methanogenic species that use acetic acid as an electron donor (Fan *et al.* 2022). Hydrogenedentes can syntrophically degrade glycerol and lipids by expressing genes encoding triacylglycerol extracellular hydrolysis (Nobu *et al.* 2015; Gaspari *et al.* 2023). The relative abundances of Halobacterota in BC25, BC50, BC75, and BC100 increased by 100.69, 242.16, 130.79, and 558.11%, respectively, while that of Hydrogenedentes in BC25, BC50, BC75, and BC100 increased by 90.00, 80.00, 100.00, and 400.00%, respectively, compared with that in BC00. Spirochaetota can convert carbohydrates into volatile fatty acids (Yang *et al.* 2020a, 2020b; Borth *et al.* 2022). The relative abundance of Spirochaetota in BC25, BC50, BC75, and BC100 increased by 303.11, 271.79, 332.81, and 146.51%, respectively, compared with that in BC00. Synergistota plays an important role in the acidification process of anaerobic digestion (Park *et al.* 2016). The relative abundance of Synergistota in BC25, BC50, BC75, and BC100 increased by 146.15, 81.45, 88.69, and 375.57%, respectively, compared with that in BC00.

Bathyarchaeia, *Methanobacterium*, *Methanoculleus*, *Methanolinea*, *Methanomassiliicoccus*, *Methanomethylovorans*, *Methanomicrobium*, *Methanosaeta*, *Methanosarcina*, and *Methanospirillumm* were dominant methanogenic archaea, and their relative abundances in different samples were 94.14% (BC00), 86.59% (BC25), 89.75% (BC50), 89.07% (BC75), and 89.45% (BC100), respectively. *Bathyarchaeia* is a multifunctional methanogenic archaeon that can promote the degradation of carbohydrates, proteins, volatile fatty acids, and methyl compounds and use H_2 and CO_2 to synthesize acetate and lactate (Khan *et al.* 2022). *Bathyarchaeia* could also enhance the activity of methyl coenzyme M and accelerate methanogenesis

(Li *et al.* 2021). The relative abundance of *Bathyarchaeia* in BC25, BC50, BC75, and BC100 increased by 457.14, 361.68, 188.89, and 659.18%, respectively, compared with that in BC00. *Methanobacterium* (Jing *et al.* 2017), *Methanoculleus* (Dong *et al.* 2022), and *Methanospirillum* (Zhou *et al.* 2014) are hydrogenotrophic methanogenics that can consume H_2 with CO_2 or formic acid to produce methane. The relative abundances of *Methanobacterium*, *Methanoculleus,* and *Methanospirillum* in BC100 increased by 66.31, 1430.77, and 261.36%, respectively, compared with that in BC00. *Methanolinea* can produce methane primarily from H_2 and formic acid as substrates (Li *et al.* 2018b), and its relative abundances in BC100 increased by 58.13% compared with that in BC00. *Methanomassiliicoccus* is a methyl methanogenic bacterium that can produce methane primarily from methanol (or methylamine) with hydrogen as an electron donor (Becker *et al.* 2016). The relative abundances of *Methanomassiliicoccus* in BC100 increased by 112.90% compared with that in BC00. The addition of biochar increased the relative abundance of *Methanomicrobium* and *Methanosaeta*. In BC25, BC50, BC75, and BC100, the relative abundances of *Methanomicrobium* increased by 80.00, 60.00, 160.00, and 400.00%, respectively, compared with that in BC00. *Methanosaeta* could participate in the DIET by receiving electrons directly from bioelectric connections or by some conductive materials directly accepting electrons to produce methane (Zhao *et al.* 2018; Zhang *et al.* 2020). And the relative abundances of *Methanosaeta* increased by 14.68% compared with BC00.

BC-I represented various bacteria in initial inoculation sludge; BC00, BC25, BC50, BC75, and BC100 represented bacteria in mixed culture with biochar dosages of 0, 2.5, 5.0, 7.5, and 10.0 g/L, respectively.

3.2.4. Functional genes of PICRUSt metabolism

Figure 6 shows the four main functional genes of KEGG of archaea, including metabolism (71.26–75.49%), genetic information processing (20.90–24.73%), environmental information processing (1.33–1.78%), and cellular process (1.65–2.44%). The secondary metabolic pathways of metabolism mainly included amino acid metabolism, the metabolism of cofactors and vitamins, and carbohydrate metabolism. Moreover, the relative abundances of functional genes related to amino acid metabolism in BC25 and BC75 increased by 4.99 and 4.97%, respectively, compared with that in BC00. The relative abundances of genes related to cofactors and vitamin metabolism in BC25, BC50, BC75, and BC100 increased by 6.61, 11.72, 7.38, and 16.67%, respectively, compared with that in BC00. The relative abundances of genes related to carbohydrate metabolism in BC25, BC50, and BC100 increased by 3.49, 6.25, and 3.63%, respectively, compared with that in BC00. The secondary metabolic pathways of genetic information processing were mainly replication and repair, folding, sorting and

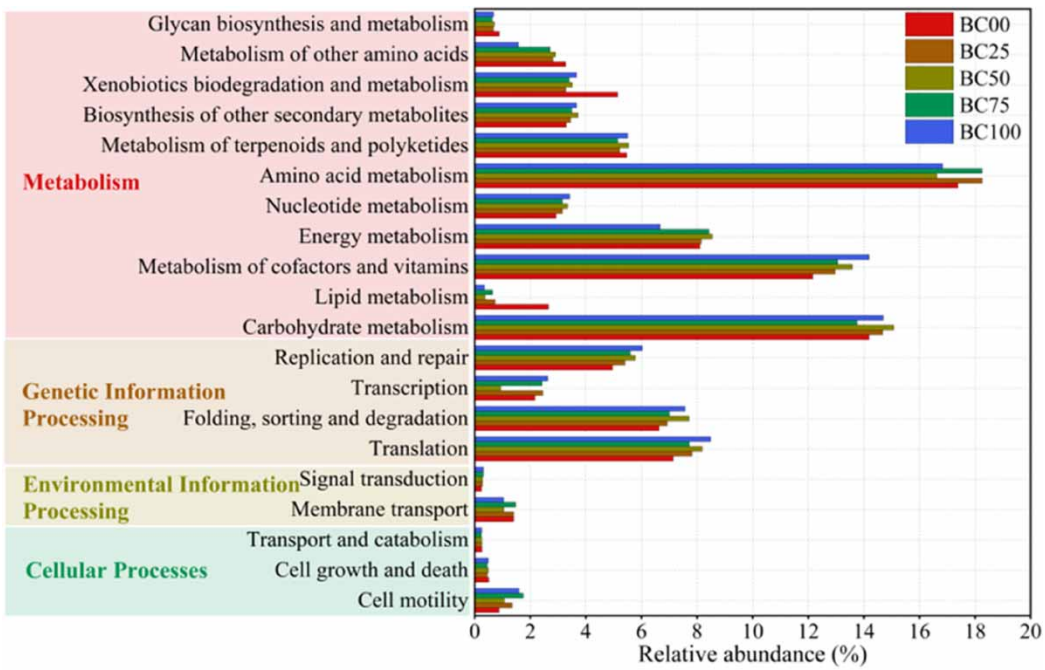

Figure 6 | Relative abundance of KEGG pathway level 2 in archaea.

degradation, and translation. The relative abundance of genes related to replication and repair in BC25, BC50, BC75, and BC100 increased by 8.93, 16.41, 12.80, and 21.54%, respectively, compared with that in BC00. The relative abundance of genes related to folding, sorting, and degradation in BC25, BC50, BC75, and BC100 increased by 4.41, 16.38, 5.65, and 14.16%, respectively, compared with that in BC00. The relative abundance of genes related to translation in BC25, BC50, BC75, and BC100 increased by 9.44, 14.59, 8.17, and 18.84%, respectively, compared with that in BC00. The secondary metabolic pathways of environmental information processing were mainly signal transduction and membrane transport. The relative abundance of genes related to signal transduction in BC25, BC50, BC75, and BC100 increased by 12.05, 12.99, 24.66, and 25.49%, respectively, compared with that in BC00. The relative abundance of genes related to membrane transport in BC75 increased by 5.14%, respectively, compared with that in BC00. Cellular processes are mainly involved cell motility, and the relative abundance of genes related to it in BC25, BC50, BC75, and BC100 increased by 54.18, 22.06, 99.55, and 82.00%, respectively, compared with that in BC00.

As carbohydrates and amino acids are the most important components of food waste, the differences in the relative abundances of functional genes related to carbohydrate metabolism and amino acid metabolism were investigated. It can be seen from Figure 7 that the relative abundances of genes related to C5-branched dibasic acid metabolism, pyruvate metabolism, citrate cycle (TCA cycle), and glycolysis/gluconeogenesis were highest in BC100, which were 11.38–26.27% higher than those in BC00. The relative abundances of genes related to histidine metabolism, lysine biosynthesis, and valine, leucine,

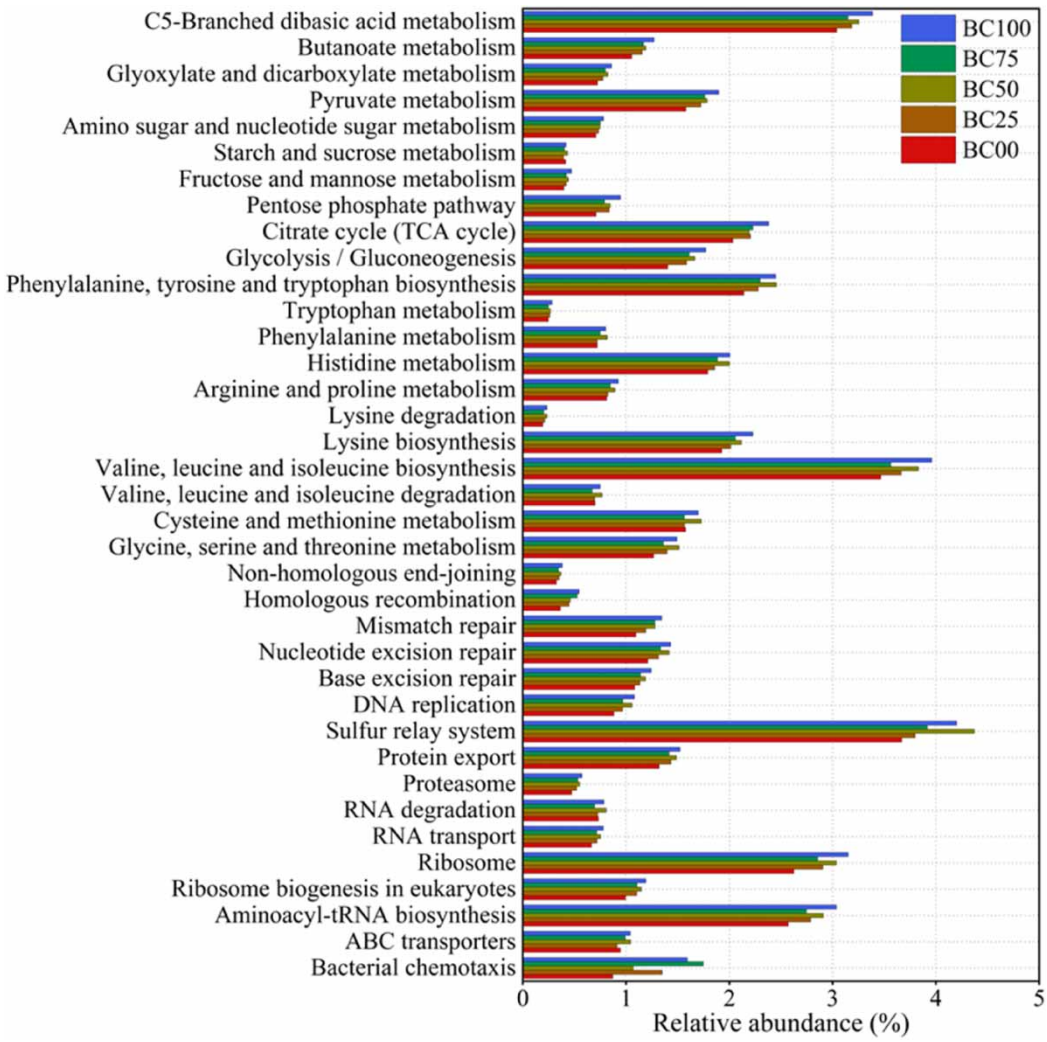

Figure 7 | Relative abundance of KEGG pathway level 3 in archaea.

and isoleucine biosynthesis were also highest in BC100, which were 11.96–15.71% higher than those in BC00. The relative abundance of genes related to phenylalanine, tyrosine, and tryptophan biosynthesis was highest in BC50, followed by BC100. The addition of biochar with 10 g/L increased the relative abundance of functional genes related to carbohydrate and amino acid metabolism. This may be related to *Bathyarchaeia*, which can increase the activity of methyl coenzyme M and promote the degradation of organic matter, such as carbohydrates and proteins (Li *et al.* 2021; Khan *et al.* 2022). Their abundance increased by 659.18% in the BC100 experimental group compared with the control group (Figure 5).

As the processing of genetic information and environmental information can ensure the transfer of information within or between species, the differences in the relative abundance of functional genes for replication and repair, folding, sorting and degradation, translation, membrane transport, and cell motility were analyzed. The relative abundances of genes related to mismatch repair, nucleotide excision repair, and base excision repair were highest in BC100, which were 14.76–22.76% higher than those in BC00. The relative abundances of genes related to the sulfur relay system and protein export were also highest in BC100, which were 14.47 and 15.40% higher than those in BC00, respectively. The relative abundances of genes related to ribosome and aminoacyl-tRNA biosynthesis were also highest in BC100, which were 19.95 and 18.15% higher than those in BC00, respectively. The relative abundance of ABC transporters was highest in BC50, followed by BC100, which was 10.44 and 10.02% higher than that in BC00, respectively. The relative abundance of genes related to bacterial chemotaxis was highest in BC75, followed by BC100, which were 100.76 and 83.09% higher than those in BC00, respectively. The results indicate that biochar addition with 10.0 g/L could promote metabolism and genetic information processing.

4. CONCLUSION

Biochar addition with different dosages could increase the cumulative methane production by 15.70–128.38%, with an optimal biochar dosage of 10.00 g/L. The methanogenesis performance was significantly improved due to the increase in major carbohydrate and amino acid metabolism and the selective enrichment of *Bathyarchaeia*, *Methanobacterium*, *Methanolinea*, *Methanoculleus,* and *Methanospirillum*. Meanwhile, it could also promote microbial replication and repair, folding, sorting, and degradation, ABC transporters, and bacterial chemotaxis by the microorganisms.

AUTHOR CONTRIBUTIONS

All authors contributed to the study's conception and design. Material preparation, data collection, and analysis were performed by S.P., F.L., C.Q., J.L., and N.L.. The first draft of the manuscript was written by S.P., F.L., C.Q., and J.L., and all authors commented on previous versions of the manuscript. All authors read and approved the final manuscript.

FUNDING

This work was supported by the National Natural Science Foundation of China (No. 51908398), and the Major Science and Technology Program for Water Pollution Control and Treatment of China (2017ZX07106001).

DATA AVAILABILITY STATEMENT

All relevant data are included in the paper or its Supplementary Information.

CONFLICT OF INTEREST

The authors declare there is no conflict.

REFERENCES

Altamirano-Corona, M. F., Anaya-Reza, O. & Durán-Moreno, A. 2021 Biostimulation of food waste anaerobic digestion supplemented with granular activated carbon, biochar and magnetite: A comparative analysis. *Biomass & Bioenergy* **149**. https://doi.org/10.1016/j.biombioe.2021.106105.

Bagul, S. Y., Bharti, K., & Dhar, R. & W, D. 2017 Assessing biodiesel quality parameters for wastewater grown *Chlorella* sp. *Water Science and Technology* **76** (3), 719–727. https://doi.org/10.2166/wst.2017.223.

Becker, K. W., Elling, F. J., Yoshinaga, M. Y., Soellinger, A., Urich, T. & Hinrichs, K. 2016 Unusual butane- and pentanetriol-based tetraether lipids in *Methanomassiliicoccus luminyensis*, a representative of the seventh order of methanogens. *Applied and Environmental Microbiology* **82** (15), 4505–4516. https://doi.org/10.1128/AEM.00772-16.

Binh, Q. A. & Kajitvichyanukul, P. 2019 Adsorption mechanism of dichlorvos onto coconut fibre biochar: The significant dependence of H-bonding and the pore-filling mechanism. *Water Science and Technology* **79** (5), 866–876. https://doi.org/10.2166/wst.2018.529.

Borth, P. L. B., Perin, J. K. H., Torrecilhas, A. R., Lopes, D. D., Santos, S. C., Kuroda, E. K. & Fernandes, F. 2022 Pilot-scale anaerobic co-digestion of food and garden waste: Methane potential, performance and microbial analysis. *Biomass & Bioenergy* **157**, 106331. https://doi.org/10.1016/j.biombioe.2021.106331.

Chen, L., Fang, W., Liang, J. S., Nabi, M., Cai, Y. J., Wang, Q. Y., Zhang, P. Y. & Zhang, G. M. 2023 Biochar application in anaerobic digestion: Performances, mechanisms, environmental assessment and circular economy. *Resources Conservation and Recycling* **188**, 106720. https://doi.org/10.1016/j.resconrec.2022.106720.

Cui, Y. X., Mao, F. J., Zhang, J. X., He, Y. L., Tong, Y. W. & Peng, Y. H. 2021 Biochar enhanced high-solid mesophilic anaerobic digestion of food waste: Cell viability and methanogenic pathways. *Chemosphere* **272**, 129863. https://doi.org/10.1016/j.chemosphere.2021.129863.

Das, D. D., Schnitzer, M. I., Monreal, C. M. & Mayer, P. 2009 Chemical composition of acid–base fractions separated from biooil derived by fast pyrolysis of chicken manure. *Bioresource Technology* **100** (24), 6524–6532. https://doi.org/10.1016/j.biortech.2009.06.104.

Das, S. K., Ghosh, G. K., Avasthe, R. K. & Sinha, K. 2021 Compositional heterogeneity of different biochar: Effect of pyrolysis temperature and feedstocks. *Journal of Environmental Management* **278, Pt2**. https://doi.org/10.1016/j.jenvman.2020.111501.

Devi, M. K., Manikandan, S., Kumar, P. S., Yaashikaa, P. R., Oviyapriya, M. & Rangasamy, G. 2023 A comprehensive review on current trends and development of biomethane production from food waste: Circular economy and techno economic analysis. *Fuel* **351**, 128963. https://doi.org/10.1016/j.fuel.2023.128963.

Dong, H. Q., Cheng, J., Li, H., Yue, L. C., Xia, R. X. & Zhou, J. H. 2022 Electron transfer from *Geobacter sulfurreducens* to mixed methanogens improved methane production with feedstock gases of H_2 and CO_2. *Bioresource Technology* **347**, 126680. https://doi.org/10.1016/j.biortech.2022.126680.

Fan, Q. W., Fan, X. J., Fu, P., Sun, Y. M., Li, Y., Long, S. L., Guo, T. Y., Zheng, L., Yang, K. & Hua, D. L. 2022 Microbial community evolution, interaction, and functional genes prediction during anaerobic digestion in the presence of refractory organics. *Journal of Environmental Chemical Engineering* **10**, 3. https://doi.org/10.1016/j.jece.2022.107789.

Fisgativa, H., Tremier, A. & Dabert, P. 2016 Characterizing the variability of food waste quality: A need for efficient valorisation through anaerobic digestion. *Waste Management* **50**, 264–274. https://doi.org/10.1016/j.wasman.2016.01.041.

Gaspari, M., Treu, L., Centurion, V. B., Kotsopoulos, T. A., Campanaro, S. & Kougias, P. G. 2023 Impacts of long chain fatty acids injection on biogas reactors performance stability and microbial community structure and function. *Journal of Cleaner Production* **418**, 138048. https://doi.org/10.1016/j.jclepro.2023.138048.

Gu, S. Y., Zhang, W. Y., Xing, H. G., Wang, R. J., Sun, J. Y., Zhang, M. & Li, Y. 2022 The effect of anaerobic co-fermentation on acidification performance of food waste and cardboard waste. *Water Science and Technology* **85** (3), 839–850. https://doi.org/10.2166/wst.2022.002.

Hu, C. L., Zhang, W., Chen, Y. T., Ye, N., YangJi, D. W., Jia, H. Z., Shen, Y. T. & Song, M. N. 2021 Adsorption of Co(II) from aqueous solution using municipal sludge biochar modified by HNO_3. *Water Science and Technology* **84** (1), 251–261. https://doi.org/10.2166/wst.2021.199.

Jing, Y. H., Wan, J. J., Angelidaki, I., Zhang, S. C. & Luo, G. 2017 iTRAQ quantitative proteomic analysis reveals the pathways for methanation of propionate facilitated by magnetite. *Water Research* **108**, 212–221. https://doi.org/10.1016/j.watres.2016.10.077.

Kaur, G., Johnravindar, D. & Wong, J. W. C. 2020 Enhanced volatile fatty acid degradation and methane production efficiency by biochar addition in food waste-sludge co-digestion: A step towards increased organic loading efficiency in co-digestion. *Bioresource Technology* **308**, 123250. https://doi.org/10.1016/j.biortech.2020.123250.

Khan, A., Akbar, S., Okonkwo, V., Smith, C., Khan, S., Shah, A. A., Adnan, F., Ijaz, U. Z., Ahmed, S. & Badshah, M. 2022 Enrichment of the hydrogenotrophic methanogens for, in-situ biogas up-gradation by recirculation of gases and supply of hydrogen in methanogenic reactor. *Bioresource Technology* **345**, 126219. https://doi.org/10.1016/j.biortech.2021.126219.

Lam, S. S., Liew, R. K., Cheng, C. K., Rasit, N., Ooi, C. K., Ma, N. L., Ng, J. H., Lam, W. H., Chong, C. T. & Chase, H. A. 2018 Pyrolysis production of fruit peel biochar for potential use in treatment of palm oil mill effluent. *Journal of Environmental Management* **213**, 400–408. https://doi.org/10.1016/j.jenvman.2018.02.092.

Li, Y. Y., Jin, Y. Y., Borrion, A. & Li, J. H. 2018a Influence of feed/inoculum ratios and waste cooking oil content on the mesophilic anaerobic digestion of food waste. *Waste Management* **73**, 156–164. https://doi.org/10.1016/j.wasman.2017.12.027.

Li, Y., Yang, G. X., Li, L. H. & Sun, Y. M. 2018b Bioaugmentation for overloaded anaerobic digestion recovery with acid-tolerant methanogenic enrichment. *Waste Management* **79**, 744–751. https://doi.org/10.1016/j.wasman.2018.08.043.

Li, Y., Zhao, J. & Zhang, Z. H. 2021 Implementing metatranscriptomics to unveil the mechanism of bioaugmentation adopted in a continuous anaerobic process treating cow manure. *Bioresource Technology* **330**, 124962. https://doi.org/10.1016/j.biortech.2021.124962.

Lim, E. Y., Tian, H. L., Chen, Y. Y., Ni, K. W., Zhang, J. X. & Tong, Y. W. 2020 Methanogenic pathway and microbial succession during start-up and stabilization of thermophilic food waste anaerobic digestion with biochar. *Bioresource Technology* **314**, 123751. https://doi.org/10.1016/j.biortech.2020.123751.

Liu, K. L., Lv, L. Y., Li, W. G., Ren, Z. J., Wang, P. F., Liu, X. Y., Gao, W. F., Sun, L. & Zhang, G. M. 2023 A comprehensive review on food waste anaerobic co-digestion: Research progress and tendencies. *Science of the Total Environment* **878**, 163155. https://doi.org/10.1016/j.scitotenv.2023.163155.

Luo, C. H., Lü, F., Shao, L. M. & He, P. J. 2015 Application of eco-compatible biochar in anaerobic digestion to relieve acid stress and promote the selective colonization of functional microbes. *Water Research* **68**, 710–718. https://doi.org/10.1016/j.watres.2014.10.052.

Luo, L. W., Chu, P. Y., Liang, J. L., Johnravindar, D., Zhao, J. & Wong, J. W. C. 2022 Enhanced stability of food waste anaerobic digestion under low inoculum to substrate ratio by using biochar. *Environmental Technology* 1–10. https://doi.org/10.1080/09593330.2022.2157759.

Nobu, M. K., Narihiro, T., Rinke, C., Kamagata, Y., Tringe, S. G., Woyke, T. & Liu, W. T. 2015 Microbial dark matter ecogenomics reveals complex synergistic networks in a methanogenic bioreactor. *Isme Journal* **9** (8), 1710–1722. https://doi.org/10.1038/ismej.2014.256.

Pan, J. T., Ma, J. Y., Liu, X. X., Zhai, L. M., Ouyang, X. H. & Liu, H. B. 2019 Effects of different types of biochar on the anaerobic digestion of chicken manure. *Bioresource Technology* **275**, 258–265. https://doi.org/10.1016/j.biortech.2018.12.068.

Park, S., Cui, F. H., Mo, K. & Kim, M. 2016 Mathematical models and bacterial communities for ammonia toxicity in mesophilic anaerobes not acclimated to high concentrations of ammonia. *Water Science and Technology* **74** (4), 935–942. https://doi.org/10.2166/wst.2016.274.

Rasapoor, M., Young, B., Brar, R., Sarmah, A., Zhuang, W. Q. & Baroutian, S. 2020 Recognizing the challenges of anaerobic digestion: Critical steps toward improving biogas generation. *Fuel* **261**, 116497. https://doi.org/10.1016/j.fuel.2019.116497.

Rivière, D., Desvignes, V., Pelletier, E., Chaussonnerie, S., Guermazi, S., Weissenbach, J., Li, T., Camacho, P. & Sghir, A. 2009 Towards the definition of a core of microorganisms involved in anaerobic digestion of sludge. *Isme Journal* **3** (6), 700–714. https://doi.org/10.1038/ismej.2009.2.

Shanmugam, S. R., Adhikari, S., Nam, H. & Sajib, S. K. 2018 Effect of bio-char on methane generation from glucose and aqueous phase of algae liquefaction using mixed anaerobic cultures. *Biomass & Bioenergy* **108**, 479–486. https://doi.org/10.1016/j.biombioe.2017.10.034.

Shen, Y. W., Linville, J. L., Ignacio-deleon, P. A. A., Schoene, R. P. & Urgun-Demirtas, M. 2016 Towards a sustainable paradigm of waste-to-energy process: Enhanced anaerobic digestion of sludge with woody biochar. *Journal of Cleaner Production* **135**, 1054–1064. https://doi.org/10.1016/j.jclepro.2016.06.144.

Sun, T. R., Levin, B. D. A., Guzman, J. J. L., Enders, A., Muller, D. A., Angenent, L. T. & Lehmann, J. 2017 Rapid electron transfer by the carbon matrix in natural pyrogenic carbon. *Nature Communications* **8** (1), 14873. https://doi.org/10.1038/ncomms14873.

Valenzuela-Cantú, A. K., Atilano-Camino, M. M., Cervantes, F. J. & Pat Espadas, A. M. 2024 Biochar mitigates the adverse effects of antimony on methanogenic activity: Role as methane production-enhancer. *Water Science and Technology* **89** (3), 788–798. https://doi.org/10.2166/wst.2024.030.

Visiy, E. B., Djousse, B. M. K., Martin, L., Zangue, C. N., Sangodoyin, A., Gbadegesin, A. S. & Fonkou, T. 2022 Effectiveness of biochar filters vegetated with *Echinochloa pyramidalis* in domestic wastewater treatment. *Water Science and Technology* **85** (9), 2613–2624. https://doi.org/10.2166/wst.2022.147.

Wang, G. J., Gao, X., Li, Q., Zhao, H. X., Liu, Y. Z., Wang, X. C. C. & Chen, R. 2020a Redox-based electron exchange capacity of biowaste-derived biochar accelerates syntrophic phenol oxidation for methanogenesis via direct interspecies electron transfer. *Journal of Hazardous Materials* **390**, 121726. https://doi.org/10.1016/j.jhazmat.2019.121726.

Wang, P. X., Peng, H. X., Adhikari, S., Higgins, B., Roy, P., Dai, W. & Shi, X. C. 2020b Enhancement of biogas production from wastewater sludge via anaerobic digestion assisted with biochar amendment. *Bioresource Technology* **309**, 123368. https://doi.org/10.1016/j.biortech.2020.123368.

Wang, G. J., Li, Q., Yuwen, C. S., Gong, K., Sheng, L., Li, Y., Xing, Y. & Chen, R. 2021a Biochar triggers methanogenesis recovery of a severely acidified anaerobic digestion system via hydrogen-based syntrophic pathway inhibition. *International Journal of Hydrogen Energy* **46** (15), 9666–9677. https://doi.org/10.1016/j.ijhydene.2020.03.115.

Wang, J. F., Zhao, Z. Q. & Zhang, Y. B. 2021b Enhancing anaerobic digestion of kitchen wastes with biochar: Link between different properties and critical mechanisms of promoting interspecies electron transfer. *Renewable Energy* **167**, 791–799. https://doi.org/10.1016/j.renene.2020.11.153.

Wang, Y., Wei, W., Huang, Q. S. & Ni, B. J. 2021c Methane production from algae in anaerobic digestion: Role of corncob ash supplementation. *Journal of Cleaner Production* **327**, 129485. https://doi.org/10.1016/j.jclepro.2021.129485.

Xin, O. Y., Han, Y. T., Cao, X. & Chen, J. W. 2017 Magnetic biochar combining adsorption and separation recycle for removal of chromium in aqueous solution. *Water Science and Technology* **75** (5), 1177–1184. https://doi.org/10.2166/wst.2016.610.

Xu, Y. G., Bai, T. X., Yan, Y. B., Zhao, Y. F., Yuan, L., Pan, P. & Jiang, Z. 2020 Enhanced removal of hexavalent chromium by different acid-modified biochar derived from corn straw: Behavior and mechanism. *Water Science and Technology* **81** (10), 2270–2280. https://doi.org/10.2166/wst.2020.290.

Yang, B., Xu, H., Liu, Y. B., Li, F., Song, X. S., Wang, Z. W. & Sand, W. 2020a Role of GAC-MnO_2 catalyst for triggering the extracellular electron transfer and boosting CH_4 production in syntrophic methanogenesis. *Chemical Engineering Journal* **383**, 123211. https://doi.org/10.1016/j.cej.2019.123211.

Yang, Z. B., Liu, X. C., Zhang, M. D., Liu, L. X., Xu, X. X., Xian, J. R. & Cheng, Z. 2020b Effect of temperature and duration of pyrolysis on spent tea leaves biochar: Physiochemical properties and Cd(II) adsorption capacity. *Water Science and Technology* **81** (12), 2533–2544. https://doi.org/10.2166/wst.2020.309.

Yirong, C., Zhang, W., Heaven, S. & Banks, C. J. 2017 Influence of ammonia in the anaerobic digestion of food waste. *Journal of Environmental Chemical Engineering* **5** (5), 5131–5142. https://doi.org/10.1016/j.jece.2017.09.043.

Zhang, Y., Xu, X. Y., Zhang, P. Y., Zhao, L., Qiu, H. & Cao, X. D. 2019 Pyrolysis-temperature depended quinone and carbonyl groups as the electron accepting sites in barley grass derived biochar. *Chemosphere* **232**, 273–280. https://doi.org/10.1016/j.chemosphere.2019.05.225.

Zhang, J., Zhang, R. T., Wang, H. Y. & Yang, K. 2020 Direct interspecies electron transfer stimulated by granular activated carbon enhances anaerobic methanation efficiency from typical kitchen waste lipid-rapeseed oil. *Science of the Total Environment* **704**, 135282. https://doi.org/10.1016/j.scitotenv.2019.135282.

Zhao, X. L., Liu, J. H., Liu, J. J., Yang, F. Y., Zhu, W. B., Yuan, X. F., Hu, Y. G., Cui, Z. J. & Wang, X. F. 2017 Effect of ensiling and silage additives on biogas production and microbial community dynamics during anaerobic digestion of switchgrass. *Bioresource Technology* **241**, 349–359. https://doi.org/10.1016/j.biortech.2017.03.183.

Zhao, Z. S., Li, Y., Yu, Q. L. & Zhang, Y. B. 2018 Ferroferric oxide triggered possible direct interspecies electron transfer between *Syntrophomonas* and *Methanosaeta* to enhance waste activated sludge anaerobic digestion. *Bioresource Technology* **250**, 79–85. https://doi.org/10.1016/j.biortech.2017.11.003.

Zhou, L. G., Liu, X. L. & Dong, X. Z. 2014 *Methanospirillum psychrodurum* sp. nova, isolated from wetland soil. *International Journal of Systematic and Evolutionary Microbiology* **64**, 638–641. https://doi.org/10.1099/ijs.0.057299-0.

First received 3 March 2024; accepted in revised form 20 April 2024. Available online 12 June 2024